Bioorganic & Medicinal Chemistry 24 (2016) 4281–4290

Contents lists available at ScienceDirect

Bioorganic & Medicinal Chemistry

journal homepage: www.elsevier.com/locate/bmc

Discovery and optimization of a series of imidazo[4,5-*b*]pyrazine derivatives as highly potent and exquisitely selective inhibitors of the mesenchymal–epithelial transition factor (c-Met) protein kinase

Fei Zhao, Jing Zhang, Leduo Zhang, Yu Hao, Chen Shi, Guangxin Xia, Jianxin Yu *, Yanjun Liu *

Central Research Institute, Shanghai Pharmaceuticals Holding Co., Ltd, Building 5, No. 898 Halei Road, Shanghai 201203, PR China

ARTICLE INFO

Article history:
Received 26 May 2016
Revised 9 July 2016
Accepted 11 July 2016
Available online 12 July 2016

Keywords:
c-Met inhibitors
Imidazo[4,5-*b*]pyrazines
Docking study
Structure–activity relationship

ABSTRACT

Aberrant c-Met activation has been implicated in multiple tumor oncogenic processes and drug resistance. In this study, a series of imidazo[4,5-*b*]pyrazine derivatives was designed and synthesized, and their inhibitory activities were evaluated in vitro. Structure–activity relationship (SAR) was investigated systematically and docking analysis was performed to elucidate the binding mode, leading to the identification of the most promising compound **1D-2** which exhibited significant inhibitory effect on both enzymatic (IC_{50} = 1.45 nM) and cellular (IC_{50} = 24.7 nM in H1993 cell line) assays, as well as exquisite selectivity and satisfactory metabolic stability in human and rat liver microsomes.

1. Introduction

As a member of the family of receptor tyrosine kinases (RTK), mesenchymal–epithelial transition factor (c-Met) is a proto-oncogene and its endogenous ligand is hepatocyte growth factor (HGF).[1] The HGF/c-Met signaling pathway plays an important role in a variety of biological activities such as proliferation, survival and tissue repair, etc. Although these activities are essential in the development of mammalian cells, they are also implicated in cancer progression such as proliferation, invasion and metastasis.[2] In normal tissues the expression level of MET is very low, but overexpression has been found in a number of major human malignancies and was considered to be related to high tumors grade and poor prognosis.[3–6] Moreover, it was reported that the resistance of tumor cells in the course of chemotherapy, radiotherapy and other RTK based target therapy was associated with aberrant c-Met signaling and amplification of the Met has been detected in 20% of acquired resistance to epidermal growth factor receptor (EGFR) inhibitors.[7,8]

Since its central role in tumor cell biology, discovery of c-Met tyrosine kinase inhibitors especially ATP-competitive small molecule inhibitor has recently attracted much attention in targeted cancer therapies. This research was developed rapidly as a result of the report of crystal structures of c-Met in 2002 and 2003.[9,10] To date, several drug candidates acting on c-Met have been approved. **PF-02341066** (Crizotinib, developed by Pfizer Inc)[11] is a dual inhibitor of c-Met and anaplastic lymphoma kinase (ALK), and it was approved on August 26, 2011 for treatment of non-small cell lung carcinoma (NSCLC). **XL184** (Cabozantinib, developed by Exelixis Inc),[12] as a inhibitor of c-Met and VEGFR2, was approved for treatment of medullary thyroid cancer (MTC) in November 2012. In recent years, a number of different types of small molecule c-Met inhibitors were reported.[13–19] The first generation of c-Met inhibitors have broad kinase activities, while the second generation are relatively selective. Although so far none of selective inhibitors has been approved, a number of drug candidates have entered clinical trials, such as **PF4217903**,[20] **JNJ38877605**,[21] **INCB28060**,[22] etc.

As shown in Figure 1, chemically these reference compounds all share a relatively conserved structure, including a right ring of quinoline moiety ($\mathbf{P_1}$), a methylene linker, a condensed five-membered and six-membered bi-heteroaryl ring core and a hydrophilic aromatic ring side chain at the 6-position ($\mathbf{P_2}$). A survey of the literature on the binding information suggests that the molecule of the selective c-Met inhibitor makes a turn at the methylene linker and adopt a bent 'U-shaped' conformation binding mode with the inhibitor wrapped around Met-1211. There is a π–π stacking interaction between the fused ring core and the A-loop residue Tyr-1230, which is important for overall potency. The *N*-3 nitrogen of the fused ring is necessary and forms a hydrogen bond with the *N*–H of the DFG Asp-1222 residue. The side chain at the 6-position

* Corresponding authors. Tel.: +86 21 61871700; fax: +86 21 50128885.
E-mail addresses: yujx@sphchina.com (J. Yu), liuyj@sphchina.com (Y. Liu).

http://dx.doi.org/10.1016/j.bmc.2016.07.019
0968-0896/

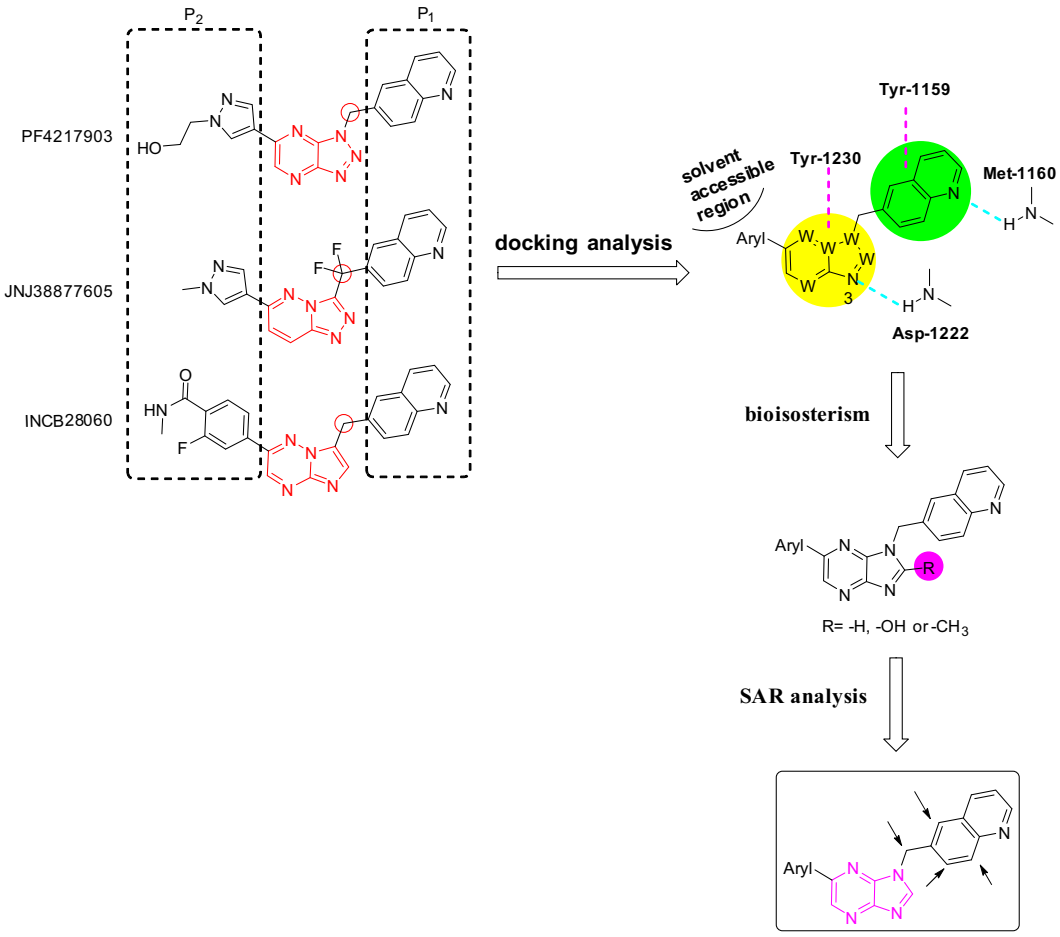

Figure 1. Design of molecular scaffolds based on known drug candidates.

was considered to direct toward the solvent-accessible region of c-Met. Besides, the quinoline is docked into the hinge region and the nitrogen atom participates in a hydrogen bond with Met-1160 and there is also a π–π stacking interaction between the aromatic quinoline ring and benzene ring of Tyr-1159.[16,20,23–25] With this binding information in mind, we hypothesized that the nitrogen at the 2-position of the fused ring is unnecessary for the binding and could be replaced. Here, we wish to efficiently identify a series of potent and selective c-Met inhibitors. To this end, we maintained the quinoline moiety as well as the 1-methyl-1*H*-4-pyrazole substituent at the 6-position of the fused ring which is usually used in active c-Met inhibitors, while taking imidazo[4,5-*b*]pyrazine as the core structure by means of bioisosteric replacement and introducing different substituents such as methyl group or hydroxyl group at the 2-position to investigate the influence on the activity preliminarily. In addition, further optimization of the active scaffold in order to improve the potency in both enzymatic and cellular assays was also investigated and the exploration was mainly focused on the methylene linker and quinoline moiety.

2. Results and discussion

2.1. Chemistry

Outlined in Scheme 1 is the synthesis of title compounds **1**–**5**. A reaction of 2-amino-3,5-dibromopyrazine (**a**) with quinolin-6-ylmethanamine (**b1**) in the presence of *N*,*N*-diisopropyl ethylamine (DIPEA) afforded intermediate 6-bromo-N^2-(quinolin-6-ylmethyl) pyrazine-2,3-diamine (**c1**). Subsequently **c1** was treated with HOAc and $POCl_3$ to give 6-((6-bromo-2-methyl-1*H*-imidazo[4,5-*b*]pyrazin-1-yl)methyl)quinoline (**d**), followed by Suzuki coupling with 1-methyl-4-(4,4,5,5-tetramethyl-1,3,2-dioxaborolan-2-yl)-1*H*-pyrazole to provide compound **1**. When **c1** reacted with CDI, 6-bromo-1-(quinolin-6-ylmethyl)-1*H*-imidazo[4,5-*b*]pyrazin-2-ol (**e**) was obtained, which was subjected to Suzuki coupling with corresponding boric acid or boric acid ester to produce compounds **2**–**4**. Preparation of compound **5** was accomplished in a similar manner to compounds **1**–**4** using the corresponding intermediate 6-((6-bromo-1*H*-imidazo[4,5-*b*]pyrazin-1-yl)methyl) quinoline (**f1**), which was prepared from the reaction of intermediate **c1** with diethoxymethyl acetate.

All the other title compounds (**6**–**27**, **1C**–**10G**) were synthesized by a procedure similar to that described for the synthesis of compound **5** using corresponding boric acid or boric acid ester reacted with corresponding intermediate **f1**–**f9** which was prepared from a series of different substituted amines **b1**–**b9** (synthetic procedures see Supplementary material) as a starting material (Scheme 2).

2.2. Biological evaluation

In the early studies, compounds **1**–**5** were firstly synthesized and their ability to inhibit the c-Met kinase and non-small cell lung cancer cell line H1993 in vitro were measured. As shown in Table 1, only compound **5** (6-((6-(1-methyl-1*H*-pyrazol-4-yl)-1*H*-imidazo[4,5-*b*]pyrazin-1-yl)methyl)quinoline) demonstrated moderate biochemical potency toward c-Met with an IC_{50} value of 9.9 nM and possessed inhibitory activity on H1993 cell line with an IC_{50} value of 0.617 μM. All the other compounds displayed quite weak

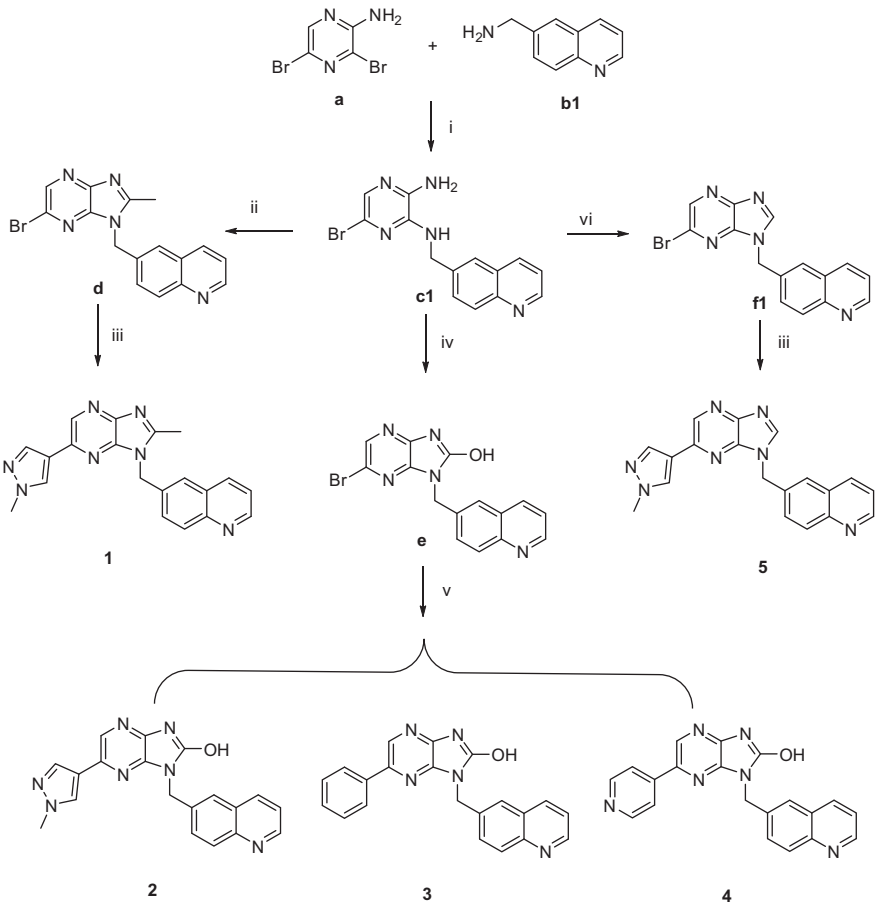

Scheme 1. Reagents and conditions: (i) DIPEA, NMP, 180 °C, 12 h; (ii) HOAc, $POCl_3$, reflux, 4 h; (iii) 1-methyl-4-(4,4,5,5-tetramethyl-1,3,2-dioxaborolan-2-yl)-1*H*-pyrazole, Pd$(dppf)_2Cl_2$·DCM complex, K_2CO_3, dioxane, H_2O, 110 °C, 4 h; (iv) CDI, dioxane, reflux, overnight; (v) corresponding boric acid or boric acid ester, Pd$(dppf)_2Cl_2$·DCM complex, K_2CO_3, dioxane, H_2O, 110 °C, 4 h; (vi) diethoxymethyl acetate, 150 °C, 12 h.

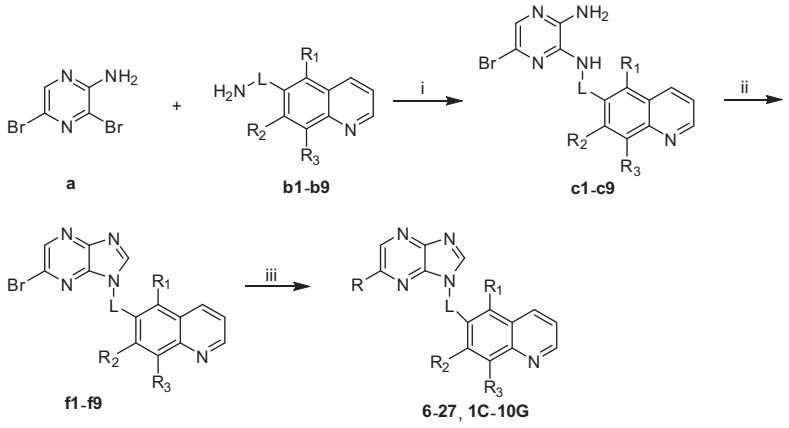

R_1, R_2=H, F, or $–CH_3$; R_3=H or F; L=-CH_2- or $–CH(CH_3)$- or $–CH(CH_2CH_3)$-

Scheme 2. Reagents and conditions: (i) DIPEA, NMP, 180 °C, overnight; (ii) diethoxymethyl acetate, 150 °C, 12 h; (iii) corresponding boric acid or boric acid ester, Pd$(dppf)_2Cl_2$·DCM complex, K_2CO_3, dioxane, H_2O, 110 °C, 4 h.

or almost no inhibitory activity toward c-Met. We can conclude that the core structure has a great effect on the inhibitory activity, and the introduction of methyl group or hydroxyl group at the 2-position of imidazole can lead to the loss of c-Met inhibitory potency. Therefore compound **5** was selected as an attractive starting point in the next study for chemistry optimization and structure–activity relationship (SAR) exploration to gain further insight on the potential of this structural class.

Thus, we synthesized eleven compounds (**6**–**16**) varied by different substituents at the 6-position of the imidazo[4,5-*b*]pyrazine core ring to investigate their inhibitory activities. As shown in Table 2, all these compounds demonstrated c-Met inhibitory

Table 1
SAR of the core

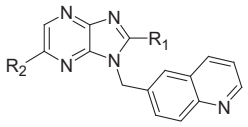

Compd	R_1	R_2	Enzyme IC_{50}[a] (nM)	H1993[b] IC_{50}[a] (μM)
1	$-CH_3$	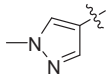	640.9	>10
2	–OH	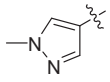	>1000	>10
3	–OH	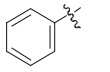	>1000	>10
4	–OH	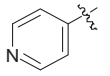	>1000	>10
5	–H	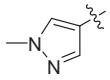	9.9	0.617
Control	PF4217903		0.3	0.034

[a] IC_{50} are based on triple runs of experiments.
[b] H1993: human non-small-cell lung cancer cell line with c-Met overexpression.

activities with IC_{50} values ranging between 12 and 81 nM, which support our previous molecular design. Besides, this result suggested that the property of the substituent at the 6-position had a certain degree of influence on the activity. It looks like the introduction of heteroaryl groups can improve the inhibitory activity.

It reported that around the methylene group of inhibitor there is a hydrophobic pocket with Leu-1157, Lys-1110, and Val-1092 residues and a small hydrophobic group on the methylene group may fit into the pocket well and form hydrophobic interaction to potentially improve the potency.[23] Taking in consideration the significance of the group on the methylene linker, compounds of type **B** were synthesized. Meanwhile, the substituents at the 6-position that taken into consideration were mainly heteroaryl groups, aryl groups and non aromatic ring based on the results of type **A**. As shown in Table 3, all these compounds exhibited relatively potent inhibition in both enzymatic and cellular assays especially for compounds **17**, **19**–**21** and **24**–**26** (IC_{50} < 1 μM in H1993 cell line). This result was encouraging since an unexpectedly significant increase in cellular activity was obtained by the addition of a methyl group. For example, compounds **17**, **19** and **20** inhibited 3-fold, 5-fold and 15-fold more potently than their corresponding compounds of unbranched type **A**, respectively. The influence of substituents at the 6-position on the activity is consistent with that of type **A**. However, great efforts should be made when compared with the positive control, which is 7-fold more potent in the enzymatic assay and nearly 6-fold more potent in the cellular assay than our most potent compound **17**.

In an ongoing effort to further improve the potency, chemistry optimization was carried out as follows. Considering the potent activities of type **B** and the possible oxidative metabolism of the methylene,[26,27] the methyl group on the linker was maintained in the follow-up study, and ethyl group was also investigated. The selected substituents at the 6-position were mainly heteroaryl groups and aryl groups. On the other hand, we turned our attention to the quinoline moiety. It is generally accepted that this structure is significant for potency and c-Met selectivity, and there is a π–π stacking interaction between the aromatic quinoline ring and benzene ring of Tyr-1159. We realized that there is still room for further improvement of potency by enhancing this stacking interaction. Some strong electron-withdrawing groups were considered to introduce to this moiety. It is well known that fluorine atom was widely used in drug design due to its special characterization and many anti-cancer drugs contained fluorine atom, such as 5-FU and Gefitinib, etc. In the next work, fluorine atom was introduced to different positions of quinoline moiety to alter the electron density in the ring with the hope of increased potency. Instead of fluorine atom, methyl group was also investigated. Therefore, other seven types of compounds (**C**–**I**) were designed and synthesized.

As Table 4 shows, many of these compounds exhibited better activities in both enzymatic and cellular assays. The inhibitory activities could improve significantly after introduction of a methyl group on the bridging methylene group as we originally designed. However, the corresponding compounds of type **E** and **F** displayed quite weak inhibitory activities (activities in the cellular assay were not tested). It can be inferred that the size of the introduced group is crucial for the activity. In order to explore the reason, compound **17** and its analogue which was introduced an ethyl

Table 2
SAR about the derivatives of type **A**

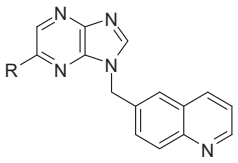

Compd	R	Enzyme IC_{50}[a] (nM)	H1993 IC_{50}[a] (μM)
6	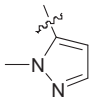	66.59	7.909
7	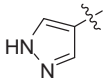	13.25	2.893
8	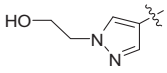	15.94	2.325
9	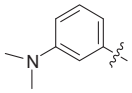	39.96	>10
10	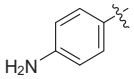	12.37	4.948
11		17.53	1.159
12		17.57	7.488
13	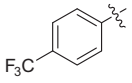	27.91	>10
14	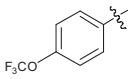	81.24	>10
15		24.59	>10
16	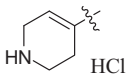	33.24	6.661
Control	PF4217903	0.33	0.034

[a] IC_{50} are based on triple runs of experiments.

Table 3
SAR about the derivatives of type **B**

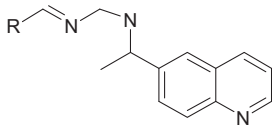

Compd	R	Enzyme IC_{50}[a] (nM)	H1993 IC_{50}[a] (μM)
17	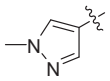	2.49	0.197
18	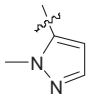	38.45	3.285
19		11.40	0.519
20	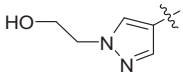	12.71	0.148
21		3.67	0.614
22		5.17	1.220
23	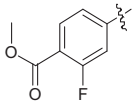	6.41	1.109
24	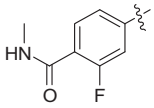	3.95	0.191
25	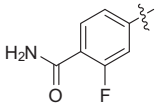	2.74	0.238
26	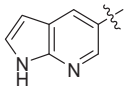	3.30	0.956
27	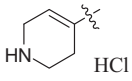	15.19	2.661
Control	PF4217903	0.33	0.034

[a] IC_{50} are based on triple runs of experiments.

group on the methylene linker were docked into the active site of c-Met. As shown in Figure 2, the two compounds adopted the similar binding mode with nonphosphorylated c-Met, however, the binding orientation was changed to some extent after introduction of a bigger ethyl group. Unlike compound **17**, the π–π stacking interaction of Tyr-1230 with the pyrazole ring was disappeared and there was an unfavorable acceptor–acceptor interaction of Arg-1208 with the *N*-4 on the pyrazine ring (displayed as red dashed line) between this analogue and kinase. For now, it looks that methyl group is the best substituent.

Another conclusion can be inferred is that the introduction of fluorine atom on the quinoline moiety can improve the activities in both enzymatic and cellular assays, but it depends on the substituted position. The introduction of a fluorine atom at the 8-position (type **C**) led to the loss of activity with $IC_{50} > 10$ μM in H1993 cell line. However, a dramatic increase in inhibitory potency in both assays was achieved after moving fluorine atom to 7-position, as illustrated with type **D**. All compounds of this type demonstrated high potency toward c-Met with $IC_{50} < 5$ nM, and several compounds exhibited potent activities in cellular assay at a double-digit nanomolar level. Compounds **1D**, **7D** and **8D** even showed more potent activities than positive control. When both 5-position and 7-position were substituted with fluorine atom (type **G**), the inhibitory activity was further improved since almost all compounds exhibited much more potent activity in both enzymatic ($IC_{50} < 2$ nM except for compounds **6G** and **10G**) and cellular assays ($IC_{50} < 85$ nM in H1993 cell line except for compounds **4G**, **5G** and **10G**). But when 5-position or 7-position was substituted with a methyl group (type **H** and **I**), the resulting compounds displayed weak inhibitory activities especially in cellular assay ($IC_{50} > 0.5$ μM except for compounds **1H** and **9H**), and it seems compounds of type **I** exhibited more weak activities in enzymatic assay than type **H**. This result is basically consistent with our prediction. The docking study of compound **1D** revealed that there was an extra weak hydrogen bond between 7-F and hydrogen atom at the 2-position of core ring, which is beneficial to the stability of binding conformation. However, this intramolecular interaction was disappeared when fluorine atom was substituted for methyl group. For compound **1G**, besides the weak hydrogen bond (displayed as green dashed line) mentioned in compound **1D**, there were an extra halogen bond between 5-F and *N*-7 of pyrazine ring (displayed as blue dashed line) and a Pi–anion interaction between pyrazole ring and Asp-1164 (displayed as orange dashed line). All these interactions are beneficial to the stability (Fig. 3). These docking results were in good agreement with our experimental results.

For the same type, the kind of substituents at the 6-position of core ring could influence the activities to some degree. The activities were quite potent when the substituents were heteroaryl groups, which is in accordance with the previous result. The activities in cellular assay were reduced or even loss when the substituent was phenyl group (**5C**–**5G**), even though some compounds demonstrated quite potent c-Met kinase inhibitory activities. It also can be inferred that the introduction of nitrogen atom could improve the potency, and compounds with *N*-monomethylated amide showed relatively weak activities than compounds with nonsubstituted amide.

Given their excellent activities in both assays, several compounds of type **D** and **G** were selected to further evaluate, including metabolic stabilities in human and rat liver microsomes (HLM and RLM), direct inhibition (DI) and time-dependent inhibition (TDI) on 5CYPs in HLM. As shown in Table 5, compounds **6D** and **6G** were unstable in both HLM and RLM probably because of the instability of ester group on benzene ring. Compound **9G** was relatively unstable in RLM, which indicate species difference. The rest compounds were stable in both HLM and RLM. Compound **9G** demonstrated both DI and TDI on most of the 5CYPs. Almost all of the compounds (include positive control) displayed DI on CYP2C9 except for compound **1D**, and this compound did not show DI or TDI on 5CYPs. It can be found that there is no obvious connection between the inhibition on 5CYPs and the number of fluorine atoms, but the kind of substituents at the 6-position has some influences in the inhibition on 5CYPs especially for the DI. The cell membrane permeability of compounds **1D**, **7D** and **8D** in Caco-2 cell model was also tested (see Supplementary material). All the selected compounds displayed high permeability with $Papp > 10 \times 10^{-6}$ cm/s and there were no efflux transporters involved (efflux ratio <2).

Through a comprehensive comparison, compounds **1D** and **8D** were selected for further evaluation. It is worth to mention that, in previous docking study on compound **1D**, we found there was some difference in the binding mode between these two configurations. The weak hydrogen bond between 7-F and hydrogen atom at the 2-position of core ring which is beneficial to the stability of binding conformation for compound (*S*)-**1D** was disappeared in

Table 4
SAR about the derivatives of types **C–I**

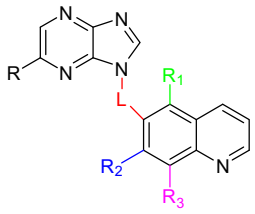

C: R_1=R_2=H, R_3=F; L=-CH(CH_3)-
D: R_1=R_3=H, R_2=F; L=-CH(CH_3)-
E: R_1=R_3=H, R_2=F; L=-CH(CH_2CH_3)-
F: R_1=F, R_2=R_3=H; L=-CH(CH_2CH_3)-
G: R_1=R_2=F, R_3=H; L=-CH(CH_3)-
H: R_1=CH_3, R_2=R_3=H; L=-CH(CH_3)-
I: R_1=R_3=H, R_2=CH_3; L=-CH(CH_3)-

Compd	R	Enzyme IC_{50}[a] (nM)	H1993 IC_{50}[a] (nM)	Compd	R	Enzyme IC_{50}[a] (nM)	H1993 IC_{50}[a] (nM)
1C	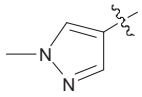	91.8	>10,000	**5F**		81.0	–[b]
1D		1.6	31.3	**5G**		1.8	513.9
1E		10.6	–[b]				
1F		13.5	–[b]	**6D**	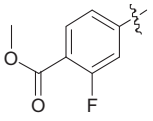	2.9	60.2
1G		1.0	35.5	**6E**		18.1	–[b]
1H		3.2	206.1	**6F**		39.2	–[b]
1I		32.6	–[b]	**6G**		4.9	29.4
				6H		5.9	–[b]
2C	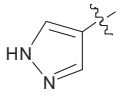	278.7	>10,000	**6I**		64.5	–[b]
2D		3.6	186.8				
2E		8.7	–[b]	**7D**	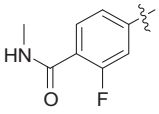	2.3	32.7
2F		37.7	–[b]	**7E**		9.4	–[b]
2H		2.7	599.1	**7F**		7.7	–[b]
				7I		31.0	–[b]
3D	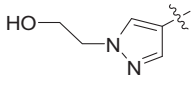	4.5	175.4				
3E		9.3	–[b]	**8D**	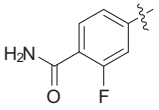	1.7	19.5
3F		22.5	–[b]	**8E**		2.5	225.8
3G		1.0	83.7	**8F**		1.6	664.8
3H		4.2	726.2	**8I**		11.7	–[b]
4C	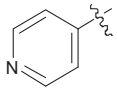	190.3	>10,000	**9C**	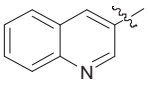	133.8	>10,000
4D		3.8	171.2	**9D**		3.4	108.8
4E		14.1	–[b]	**9E**		17.2	–[b]
4F		100.0	–[b]	**9F**		16.4	–[b]
4G		1.6	161.6	**9G**		1.3	46.1
4H		4.4	949.8	**9H**		4.9	449.9
4I		68.3	–[b]	**9I**		38.1	–[b]
5C	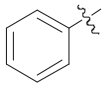	155.4	>10,000	**10C**	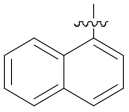	>1000	–[b]
5D		4.6	570.2	**10G**		23.8	–[b]
5E		28.1	–[b]	Control	PF4217903	0.3	33.6

[a] IC_{50} are based on triple runs of experiments.
[b] The – indicates not tested.

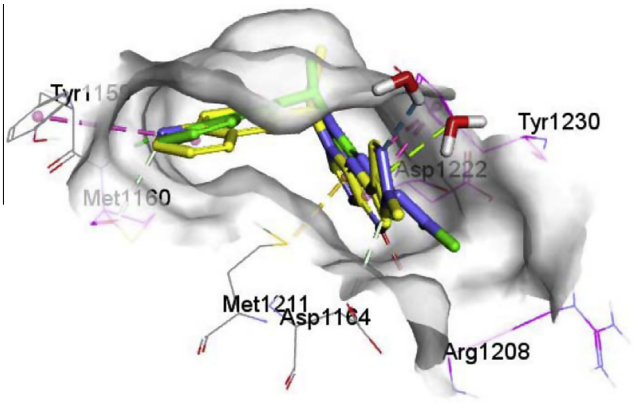

Figure 2. Overlay of compound **17** (green) and its analogue (yellow) bound with the nonphosphorylated c-Met, displaying the protein in surface representation. The residues Ile-1084, Ala-1108, Pro-1158, Tyr-1159, Met-1160, Asp-1164, Arg-1208, Met-1211, Ala-1221, Asp-1222, Ala-1226, Tyr-1230 and Asp-1231 were defined as the active site.

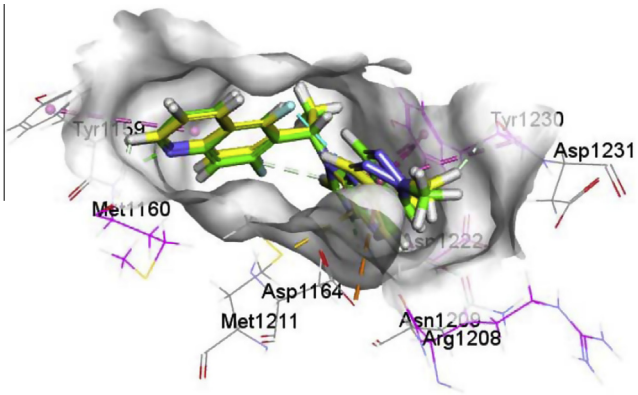

Figure 3. Overlay of compound **1D** (green) and compound **1G** (yellow) bound with the nonphosphorylated c-Met, displaying the protein in surface representation.

Table 5
Leadlikeness assessment in vitro of compounds

Compd	HLM stability[a] CL_{int} (μl/min/mg protein)	RLM stability[b] CL_{int} (μl/min/mg protein)	DI	TDI
1D	9	18	NI[c]	NI[c]
6D	73	125	2C9	NI[c]
7D	16	85	3A4, 2D6, 2C9, 2C19	3A4
8D	14	85	2C9	NI[c]
1G	11	63	2C9, 2C19	NI[c]
3G	2	10	2C9	NI[c]
4G	14	77	3A4, 2C9, 2C19	NI[c]
6G	290	179	2C9	NI[c]
9G	51	275	2D6, 2C9, 2C19	3A4, 2D6, 1A2
PF4217903	5	8	2C9	NI[c]

[a] When CL_{int} < 50 μl/min/mg protein, compound is stable in HLM.
[b] When CL_{int} < 100 μl/min/mg protein, compound is stable in RLM.[28]
[c] The NI indicates no inhibition on 5CYPs in HLM.

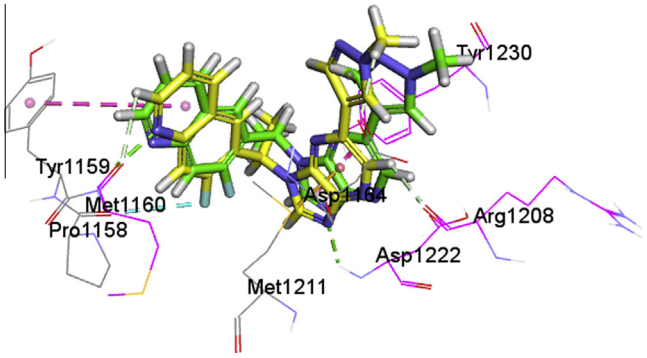

Figure 4. Overlay of compounds (*S*)-**1D** (green) and (*R*)-**1D** (yellow) bound with the nonphosphorylated c-Met.

compound (*R*)-**1D**, however, there was an extra halogen bond between 7-F of compound (*R*)-**1D** and Pro-1158 (Fig. 4, displayed as blue dashed line). This result predicted that these two compounds perhaps exhibited different activities.

Therefore, the enantiomerically pure compounds **1D-1**, **1D-2**, **8D-1** and **8D-2** were synthesized and their inhibitory activities were tested. It can be found from Table 6 that compounds with an (*S*)-configuration displayed more excellent activities than their corresponding (*R*)-configured compounds in enzymatic assays, which indicated that (*S*)-configuration was much beneficial to the binding. Unexpectedly, their activities in the cellular assay varied dramatically since compounds **1D-2** and **8D-2** showed 10-fold and 28-fold more potent activities than their enantiomers, respectively. And these two compounds all displayed more excellent activities on H1993 cell line than the positive control. We re-evaluated the metabolic stability as well as the inhibition on 5CYPs in HLM of these two compounds. Compound **1D-2** was stable in both HLM and RLM. However, compound **8D-2** was unstable in RLM, which was less stable than their racemic compound **8D**. Different from racemate **1D**, compound **1D-2** demonstrated DI on CYP2C9. Besides DI on CYP2C9, compound **8D-2** also displayed DI on CYP3A4. These two compounds all did not show TDI on 5CYPs.

Considering the high biochemical efficiency and satisfactory metabolic stability, compound **1D-2** was selected to further investigate the kinase selectivity. A panel of 18 human tyrosine kinases was selected, including highly homologous kinase AXL (tyrosine-protein kinase receptor UFO) and c-Met family member RON (macrophage-stimulating protein receptor). As expected, this compound is highly selective for c-Met, showing an IC_{50} of >1000 nM against other tested tyrosine kinases (Table 7).

3. Conclusion

In summary, what described here is the identification and rationally guided optimization process of a series of selective c-Met tyrosine kinase inhibitors with an imidazo[4,5-*b*]pyrazine scaffold by structural modification of the lead compound **5**. Many derivatives displayed potent activities in both enzymatic (at a single-digit nanomolar level) and cellular (at a double-digit nanomolar level on H1993 cell line) assays. The SAR was investigated systematically and particularly focused on the quinoline moiety, methylene linker and a range of substitutes at 6-position of the core. According to the data collected in this study, it can be concluded that the introduction of a methyl group on the methylene linker is beneficial for the activity; while the result is opposite when ethyl group was introduced instead of methyl group. The introduction of fluorine atom at quinoline moiety could improve potency except for 8-position. Molecular docking experiments were used to provide a rational explanation of the molecular

Table 6
In vitro evaluation of compounds

Compd	Configuration	Enzyme IC_{50}[a] (nM)	H1993 IC_{50}[a] (nM)	HLM stability[b] CL_{int} (μl/min/mg protein)	RLM stability[c] CL_{int} (μl/min/mg protein)	DI	TDI
1D-1	*R*	1.94	239.4	–[d]	–[d]	–[d]	–[d]
1D-2	*S*	1.45	24.7	8	49	2C9	NI[e]
8D-1	*R*	2.79	329.1	–[d]	–[d]	–[d]	–[d]
8D-2	*S*	1.32	11.8	23	131	3A4, 2C9	NI[e]
Control	PF4217903	0.33	33.6	5	8	2C9	NI[e]

[a] IC_{50} are based on triple runs of experiments.
[b] When CL_{int} < 50 μl/min/mg protein, compound is stable in HLM.
[c] When CL_{int} < 100 μl/min/mg protein, compound is stable in RLM.[28]
[d] The – indicates not tested.
[e] The NI indicates no inhibition on 5CYPs in HLM.

Table 7
Kinase-selectivity profile of compound **1D-2**

Kinase	IC_{50} (nM)	Kinase	IC_{50} (nM)
AXL	>30,000	EGFR	>30,000
RON	>30,000	EGFR [T790M]	>30,000
ALK	>30,000	ErbB4	>30,000
Flt-1	>30,000	c-Src	>30,000
VEGFR2	20,618	ABL	>30,000
c-Kit	>30,000	EphA2	>30,000
PDGFRa	27,606	EphB2	>30,000
PDGFRb	26,197	IGF1R	>30,000
RET	>30,000	FGFR1	>30,000

mechanism of the differences in activity. The analysis indicated this promotion of activity is partly owing to the contribution to maintain the stability of the favorable binding conformation through intramolecular hydrogen bond or halogen bond. This discovery verified the experimental results and had some inspiration and reference value for subsequent research. The *R*/*S* configuration had significant influence on the activity, and the compounds with an (*S*)-configuration showed more potent activity especially in cellular assay. Among all compounds tested, the most promising compound **1D-2** displayed excellent potency, satisfactory metabolic stability in both HLM and RLM as well as exquisite kinase selectivity. All these properties indicated its druggability. Further optimizations and studies on the in vivo pharmacodynamic and pharmacokinetic properties are underway in our research group and will be reported in due course.

4. Experimental

4.1. Chemistry

All reagents and solvents employed were purchased from commercial sources and used without further purification. Reactions were followed by TLC using HSGF 254 silica-gel plates (0.15–0.2 mm thickness). Silica-gel chromatography was done using the appropriate size Biotage prepacked silica filled cartridges. Melting points were determined using a WRR digital apparatus, and were uncorrected. NMR data were recorded on a *Bruker* 400 MHz or 500 MHz Digital NMR Spectrometer. Chemical shifts are expressed as δ units using tetramethylsilane as the external standard (in NMR description, s, singlet; d, doublet; t, triplet; q, quartet; m, multiplet; dd, double doublet; and br s, broad singlet). All coupling constants (*J*) are reported in Hertz. Mass spectra were measured with an Agilent quadrupole 6110 spectrometer using an ESI source coupled to an Agilent 1200 HPLC system.

The preparation of all the title compounds can be found in Supplementary material because of the limited length of the paper.

4.2. Biological evaluation

4.2.1. In vitro enzymatic assay

Inhibition of test compound on c-Met kinase activity was determined by measuring the phosphorylation level of TK substrate-biotin peptide in a Homogenous Time-Resolved Fluorescence (HTRF) assay. Into a white 384-well plate was added 2 μL/well of 5× compound in reaction buffer. Next, 4 μL of reaction buffer (50 mM HEPES pH 7.0, 0.02% NaN_3, 0.01% BSA, 0.1 mM Na_2VO_3, 5 mM $MgCl_2$ and 1 mM DTT, containing 1 μM TK substrate-biotin and 1 ng c-Met enzyme) was added to each well. After 5–10 min preincubation, the kinase reaction was initiated by the addition of 4 μL of 18 μM ATP in reaction buffer. After 30 min incubation at room temperature, the enzyme reaction was stopped by EDTA-containing buffer, which also contained europium-conjugated anti-phosphoresidue antibody and streptavidin-XL665 (SA-XL665) to allow for detection of the phosphorylated peptide product. Following 1 h incubation at room temperature fluorescence was measured with excitation of 337 nm and dual emission of 665 and 620 nm on Envision microplate reader (PerkinElmer). Signal was expressed in terms of HTRF ratio (fluorescence intensity at 665 nm/fluorescence intensity at 620 nm * 10,000).

4.2.2. In vitro growth inhibition assay

NCI-H1993 cell line was purchased from the American Type Culture Collection (ATCC, Manassas, VA, USA). Cells were maintained in RPMI 1640 media and supplemented with 10% fetal bovine serum (Gibco Life Technologies, Grand Island, NY). NCI-H1993 cells were seeded at 5000 cells/well in 96-well plates and incubated overnight. On the next day, the cells were exposed to various concentrations of compounds and further cultured for 72 h. After chromogenic reaction with Cell Counting Kit-8 (CCK-8; Dojindo Laboratories, Kumamoto, Japan), the OD450 (with reference of OD650) was measured using a Flexstation 3 reader (Molecular Devices, USA). IC_{50} values were calculated using the GraphPad Prism Software. Each experiment was carried out thrice, each time in duplicate.

4.2.3. Metabolic stability in human and rat liver microsomes

This assay utilized a 150 μl incubation system containing human or rat liver microsomes (0.5 mg/ml) to preincubate with 1 μM test compound for 5 min at 37 °C in 100 mM phosphate buffer (pH 7.4). The reactions were initiated by adding NADPH (1 mM). Midazolam was used as positive control. After 0, 5, 10 and 30 min incubations at 37 °C, the reactions were stopped by adding 300 μl acetonitrile containing tinidazole of 0.1 μg/ml as internal standard. The samples were vortexed for 10 min, and then centrifuged at 6000*g* for 10 min twice at 4 °C and an aliquot of supernatant was sampled for LC–MS/MS analysis. Calculate the CL_{int} (μl/min/mg protein) by determining the relative quantity of test compounds.

4.2.4. Direct inhibition on 5CYPs in HLM

This assay utilized a 100 μl incubation system containing human liver microsomes (0.2 mg/ml), substrate mixture (Midazolam 10 μM, Testosterone 100 μM, Dextromethophan 10 μM, Diclofenac 20 μM, Phenacetin 100 μM, (*S*)-(+)-Mephenytoin 100 μM), 10 μM test compound, which were preincubated for 5 min at 37 °C in 100 mM phosphate buffer (pH 7.4). The selective inhibitors of each P450 isoform (Ketoconazole 10 μM for CYP3A4, Quinidine 10 μM for CYP2D6, Sulfaphenazole 100 μM for CYP2C9, Naphthoflavone 10 μM for CYP1A2, Tranylcypromine 1000 μM for CYP2C19) were used as positive controls. The reactions were initiated by adding NADPH (1 mM). After 20 min incubations at 37 °C, the reactions were stopped by adding 300 μl acetonitrile containing tinidazole of 0.1 μg/ml as internal standards. The samples were vortexed for 10 min, and then centrifuged at 6000*g* for 10 min twice at 4 °C and an aliquot of supernatant was sampled for LC–MS/MS analysis. Calculate the relative activity of the enzyme by determining the relative quantity of the substrate metabolites.

4.2.5. Time-dependent inhibition on 5CYPs in HLM

This assay utilized a 200 μl incubation system containing human liver microsomes (0.2 mg/ml), 10 μM test compound, which were preincubated for 0 min, 5 min, 10 min and 20 min at 37 °C after adding NADPH (1 mM) or PBS. Then the system was incubated for 10 min at 37 °C after adding 180 μl secondary incubation mixture containing NADPH (1 mM) and substrate mixture (Midazolam 5 μM, Testosterone 50 μM, Dextromethophan 5 μM, Diclofenac 10 μM, Phenacetin 50 μM, (*S*)-(+)-Mephenytoin 50 μM). The selective inhibitors of each P450 isoform (Troleandomycin 10 μM for CYP3A4, Paroxetine 10 μM for CYP2D6, Tienilic Acid 10 μM for CYP2C9, Furafylline 10 μM for CYP1A2, (*S*)-(+)-Fluoxetine 100 μM for CYP2C19) were used as positive controls. The reactions were stopped by adding 600 μl acetonitrile containing tinidazole of 0.1 μg/ml as internal standards. The samples were vortexed for 10 min, and then centrifuged at 6000*g* for 10 min twice at 4 °C and an aliquot of supernatant was sampled for LC–MS/MS analysis. Calculate the relative activity of the enzyme and K_{obs} ($*10^{-4}$/min) by determining the relative quantity of the substrate metabolites.

4.2.6. Cell membrane permeability in Caco-2 cell model

Permeability studies were conducted at 37 °C, in a medium of HBSS, pH 7.4. Before the experiments, the TEER of the Caco-2 cell monolayers was measured to determine the TEER values. Prior to the transport study, cell monolayers were washed with the transport buffer and preincubated for 10 min. Test compounds at final concentrations of 1–10 μM in HBSS were added to the apical compartment. The basolateral compartment contained only HBSS. All transport studies were conducted in the apical (A) to basolateral (B) direction. Transwells were then placed in an orbital horizontal shaker with constant stirring (100 rpm) at 37 °C for 90 min. Add 100 μL acetonitrile containing tinidazole of 0.1 μg/ml as internal standards to sample solution and shake for 10 min, then centrifuge (6000*g*, 10 min). An aliquot of supernatant was sampled for LC–MS/MS analysis. Calculate the $Papp_{(AP-BL)}$ and efflux ratio by determining the quantity of the test compound.

4.3. Molecular docking

The crystal structure of c-Met kinase in complex with **PF4217903** (PDB ID: 3ZXZ) obtained from the protein data bank was used for molecular docking with Ligandfit docking tool in Discovery Studio (DS) 2016 package. The complex structure obtained was firstly prepared using Prepare Protein protocol in Discovery Studio. The docking site was derived from the position of the **PF4217903** cocrystallized in the binding site of 3ZXZ. And all the ligands were prepared using Prepare Ligands protocol and Minimize Ligands protocol in Discovery Studio subsequently. To validate the docking method, the **PF4217903** was used to carry out the Ligandfit docking experiment. The docking results were evaluated through comparison of the best docked binding mode with the experimental one. The RMSD was used to compare differences between the atomic distances of the docked poses and the real cocrystallized pose to measure docking reliability. The RMSD of the heavy atom is only about 0.1432 Å. It indicated that the Ligandfit docking method is fit for the cMet-small molecular ligand system. The best pose was outputted on the basis of ligandscore 1 and the protein–ligand interactions. All the compounds used in the docking study are (*S*)-configuration unless otherwise stated.

Acknowledgement

We thank NeoTrident Co., Ltd for excellent docking assistance.

Supplementary data

Supplementary data associated with this article can be found, in the online version, at http://dx.doi.org/10.1016/j.bmc.2016.07.019.

References and notes

1. Bottaro, D. P.; Rubin, J. S.; Faletto, D. L.; Chan, A. M. L.; Kmiecik, T. E.; Vande Woude, G. F.; Aaronson, S. A. *Science* **1991**, *251*, 802.
2. Shinomiya, N.; Vande Woude, G. F. *Clin. Cancer Res.* **2003**, *9*, 5085.
3. Sawada, K.; Radjabi, A. E.; Shinomiya, N.; Kistner, E.; Kenny, H.; Becker, A. R.; Turkyilmaz, M. A.; Salgia, R.; Yamada, S. D.; Vande Woude, G. F.; Tretiakova, M. S.; Lengyel, E. *Cancer Res.* **2007**, *67*, 1670.
4. Ichimura, E.; Maeshima, A.; Nakajima, T.; Nakamura, T. *Jpn. J. Cancer Res.* **1996**, *87*, 1063.
5. Hiroki, K.; Wataru, Y.; Yasuhiko, K.; Hiroshi, Y.; Hisao, I.; Eiichi, T. *Biochem. Biophys. Res. Commun.* **1992**, *189*, 227.
6. Liu, C.; Park, M.; Tsao, M. S. *Oncogene* **1992**, *7*, 181.
7. Engelman, J. A.; Zejnullahu, K.; Mitsudomi, T.; Song, Y.; Hyland, C.; Park, J. O.; Lindeman, N.; Gale, C. M.; Zhao, X.; Christensen, J.; Kosaka, T.; Holmes, A. J.; Rogers, A. M.; Cappuzzo, F.; Mok, T.; Lee, C.; Johnson, B. E.; Cantley, L. C.; Janne, P. A. *Science* **2007**, *316*, 1039.
8. Liu, X. D.; Newton, R. C.; Scherle, P. A. *Trend Mol. Med.* **2010**, *16*, 37.
9. Mroczkowski, B.; McTigue, M. A.; Sarup, J.; Murray, B.W.; Hickey, M.; Parge, H.; Zhu, J. USP 277968, EP 1243596A1, 2001.
10. Schiering, N.; Knapp, S.; Marconi, M.; Flocco, M. M.; Cui, J.; Perego, R.; Rusconi, L.; Cristiani, C. *Proc. Natl. Acad. Sci. U.S.A.* **2003**, *100*, 12654.
11. Cui, J. J.; Tran-Dube, M.; Shen, H.; Nambu, M.; Kung, P. P.; Pairish, M.; Jia, L.; Meng, J.; Funk, L.; Botrous, I.; McTigue, M.; Grodsky, N.; Ryan, K.; Padrique, E.; Alton, G.; Timofeevski, S.; Yamazaki, S.; Li, Q.; Zou, H.; Christensen, J.; Mroczkowski, B.; Bender, S.; Kania, R. S.; Edwards, M. P. *J. Med. Chem.* **2011**, *54*, 6342.
12. Roy, S.; Narang, B. K.; Rastogi, S. K.; Rawal, R. K. *Anti-Cancer Agent Med. Chem.* **2015**, *15*, 37.
13. Qian, F.; Engst, S.; Yamaguchi, K.; Yu, P. W.; Won, K. A.; Mock, L.; Lou, T.; Tan, J.; Li, C.; Tam, D.; Lougheed, J.; Michael Yakes, F.; Bentzien, F.; Xu, W.; Zaks, T.; Wooster, R.; Greschock, J.; Joly, A. H. *Cancer Res.* **2009**, *69*, 8009.
14. Schroeder, G. M.; An, Y. M.; Cai, Z. W.; Chen, X. T.; Clark, C.; Cornelius, L. A. M.; Dai, J.; Gullo-Brown, J.; Gupta, A.; Henley, B.; Hunt, J. T.; Jeyaseelan, R.; Kamath, A.; Kim, K.; Lippy, J.; Lombardo, L. J.; Manne, V.; Oppenheimer, S.; Sack, J. S.; Schmidt, R. J.; Shen, G. X.; Stefanski, K.; Tokarski, J. S.; Trainor, G. L.; Wautlet, B. S.; Wei, D.; Williams, D. K.; Zhang, Y. R.; Zhang, Y. P.; Fargnoli, J.; Borzilleri, R. M. *J. Med. Chem.* **2009**, *52*, 1251.
15. Buchanan, S. G.; Hendle, J.; Lee, P. S.; Smith, C. R.; Bounaud, P. Y.; Jessen, K. A.; Tang, C. M.; Huser, N. H.; Felce, J. D.; Froning, K. J.; Peterman, M. C.; Aubol, B. E.; Gessert, S. F.; Michael Sauder, J.; Schwinn, K. D.; Russell, M.; Rooney, I. A.; Adams, J.; Leon, B. C.; Do, T. H.; Blaney, J. M.; Sprengeler, P. A.; Thompson, D. A.; Smyth, L.; Pelletier, L. A.; Atwell, S.; Holme, K.; Wasserman, S. R.; Emtage, S.; Burley, S. K.; Reich, S. H. *Mol. Cancer Ther.* **2009**, *8*, 3181.
16. Nishii, H.; Chiba, T.; Morikami, K.; Fukami, T. A.; Sakamoto, H.; Ko, K.; Koyano, H. *Bioorg. Med. Chem. Lett.* **2010**, *20*, 1405.
17. Zhang, D. Y.; Ai, J.; Liang, Z. J.; Li, C. P.; Peng, X.; Ji, Y. C.; Jiang, H. L.; Geng, M. Y.; Luo, C.; Liu, H. *Bioorg. Med. Chem.* **2012**, *20*, 5169.
18. Dorsch, D.; Schadt, O.; Stieber, F.; Meyring, M.; Gradler, U.; Bladt, F.; Friese-Hamim, M.; Knuhl, C.; Pehl, U.; Blaukat, A. *Bioorg. Med. Chem. Lett.* **2015**, *25*, 1597.
19. Qi, B. H.; Mi, B.; Zhai, X.; Xu, Z. Y.; Zhang, X. L.; Tian, Z. R.; Gong, P. *Bioorg. Med. Chem.* **2013**, *21*, 5246.

20. Cui, J. J.; McTigue, M.; Nambu, M.; Tran-Dube, M.; Pairish, M.; Shen, H.; Jia, L.; Cheng, H. M.; Hoffman, J.; Le, P.; Jalaie, M.; Goetz, G. H.; Ryan, K.; Grodsky, N.; Deng, Y. L.; Parker, M.; Timofeevski, S.; Murray, B. W.; Yamazaki, S.; Aguirre, S.; Li, Q. H.; Zou, H.; Christensen, J. *J. Med. Chem.* **2012**, *55*, 8091.
21. Cui, J. J. *J. Med. Chem.* **2014**, *57*, 4427.
22. Liu, X. D.; Wang, Q.; Yang, G. J.; Marando, C.; Koblish, H. K.; Hall, L. M.; Fridman, J. S.; Behshad, E.; Wynn, R.; Li, Y.; Boer, J.; Diamond, S.; He, C. H.; Xu, M. Z.; Zhuo, J. C.; Yao, W. Q.; Newton, R. C.; Scherle, P. A. *Clin. Cancer Res.* **2011**, *17*, 7127.
23. Jia, H.; Dai, G. X.; Weng, J. Y.; Zhang, Z. L.; Wang, Q.; Zhou, F.; Jiao, L. X.; Cui, Y. M.; Ren, Y. X.; Fan, S. M.; Zhou, J. H.; Qing, W. G.; Gu, Y.; Wang, J.; Sai, Y.; Su, W. G. *J. Med. Chem.* **2014**, *57*, 7577.
24. Albrecht, B. K.; Harmange, J. C.; Bauer, D.; Berry, L.; Bode, C.; Boezio, A. A.; Chen, A.; Choquette, D.; Dussault, I.; Fridrich, C.; Hirai, S.; Hoffman, D.; Larrow, J. F.; Kaplan-Lefko, P.; Lin, J.; Lohman, J.; Long, A. M.; Moriguchi, J.; O'Connor, A.; Potashman, M. H.; Reese, M.; Rex, K.; Siegmund, A.; Shah, K.; Shimanovich, R.; Springer, S. K.; Teffera, Y.; Yang, Y. J.; Zhang, Y. H.; Bellon, S. F. *J. Med. Chem.* **2008**, *51*, 2879.
25. Ye, L. B.; Tian, Y. X.; Li, Z. H.; Jin, H.; Zhu, Z. G.; Wan, S. H.; Zhang, J. Y.; Yu, P. J.; Zhang, J. J.; Wu, S. G. *Eur. J. Med. Chem.* **2012**, *50*, 370.
26. Testa, B.; Mihailova, D. *J. Med. Chem.* **1978**, *21*, 683.
27. Smith, D. A.; Allerton, C.; Kalgutkar, A. S.; Waterbeemd, H.; Walker, D. K. In *Pharmacokinetic and Metabolism in Drug Design*; John Wiley & Sons: Hoboken, NJ, 2012; vol. 51,
28. Kerns, E. H.; Di, L. *Drug-like Properties: Concepts, Structure Design and Methods*; Elsevier: Oxford, UK, 2008. Part 3.